Mesenchymal stem cells restore local microenvironment and systemically suppress leukemia via reprogramming macrophages

Chengxiang Xia[1, 2, 3, 4, 5†], Tongjie Wang[1†], Hui Cheng[6†], Yong Dong[1, 2], Qitong Weng[1, 2], Guohuan Sun[6], Peiqing Zhou[1, 2], Kaitao Wang[4], Xiaofei Liu[1], Yang Geng[1], Shihui Ma[6], Sha Hao[6], Ling Xu[7], Yuxian Guan[1], Juan Du[1], Xin Du[8, 9], Yangqiu Li[7], Xiaofan Zhu[6], Yufang Shi[10], Sheng Xu[11], Demin Wang[12,13], Tao Cheng[6*], Jinyong Wang[1, 2, 3, 4, 5, 6*]

[1]CAS Key Laboratory of Regenerative Biology, Guangzhou Institutes of Biomedicine and Health, Chinese Academy of Sciences, Guangzhou, China; [2]Guangzhou Regenerative Medicine and Health-Guangdong Laboratory (GRMH-GDL), Guangzhou, China; [3]Guangdong Provincial Key Laboratory of Stem cell and Regenerative Medicine, Guangzhou Institutes of Biomedicine and Health, Chinese Academy of Sciences, Guangzhou, China; [4]Joint School of Life Sciences, Guangzhou Institutes of Biomedicine and Health, Guangzhou Medical University, Guangzhou, China; [5]University of Chinese Academy of Sciences, Beijing, China; [6]State Key Laboratory of Experimental Hematology, Institute of Hematology and Blood Diseases Hospital, Chinese Academy of Medical Sciences and Peking Union Medical College, Tianjin, China; [7]Department of Hematology, First Affiliated Hospital; Institute of Hematology, School of Medicine; Key Laboratory for Regenerative Medicine of Ministry of Education; Jinan University, Guangzhou, China; [8]Department of Hematology, Guangdong General Hospital/Guangdong Academy of Medical Sciences, Guangzhou, China; [9]South China University of Technology, Guangzhou, China; [10]The First Affiliated Hospital of Soochow University, State Key Laboratory of Radiation Medicine and Protection, Institutes for Translational Medicine, Soochow University, Suzhou, China; [11]National Key Laboratory of Medical Immunology & Institute of Immunology, Second Military Medical University, Shanghai, China; [12]Blood Research Institute, Versiti, Milwaukee,

24 WI, USA; [13]Biomedical Research Center of South China, College of Life Sciences, Fujian Normal

25 University, Fuzhou, China.

26 [†]Equal contributors.

27 [*]Correspondences: wang_jinyong@gibh.ac.cn (J.W.), chengtao@ihcams.ac.cn (T.C.).

Abstract

Bone marrow (BM) mesenchymal stem cells (MSCs) are critical components of the BM microenvironment and play an essential role in supporting hematopoiesis. Dysfunction of MSCs is associated with the impaired BM microenvironment that promotes leukemia development. However, whether and how restoration of the impaired BM microenvironment can inhibit leukemia development remain unknown. Using an established leukemia model and high-throughput RNA-seq analysis, we discovered functional degeneration of MSCs during leukemia progression. Importantly, intra-BM instead of systemic transfusion of donor healthy MSCs restored the BM microenvironment, thus systemically changing cytokine expression patterns, improving normal hematopoiesis, reducing tumor burden, and ultimately prolonging survival of the leukemia-bearing mice. Donor MSC treatment restored the function of host MSCs and reprogrammed host macrophages to fulfill tissue-repair function. Transfusion of MSC-reprogrammed macrophages largely recapitulated the therapeutic effects of MSCs. Further, we found that donor MSCs reprogrammed macrophages to reduce leukemia burden through autocrine effects of IL-6. Taken together, our study reveals that donor MSCs reprogram host macrophages to restore the BM microenvironment and inhibit leukemia development, thus validating local MSC application as a potentially effective therapy for leukemia.

Introduction

BM MSCs are key components of the BM stromal microenvironment, regulating homeostasis of the stromal niche and hematopoiesis[1]. Accumulating evidences uncover that dysfunction of MSCs is associated with leukemia progression. Deletion of *Dicer1* gene in MSCs leads to impaired osteogenic differentiation, thrombopenia, and secondary tumorigenesis[2]. In myeloproliferative neoplasms, the leukemia cells reprogram MSCs to support proliferation of leukemia stem cells[3]. Ablation of MSC-derived osteoblasts impairs the homeostasis of hematopoietic stem cells (HSC) and accelerates leukemogenesis in chronic myeloid leukemia[4]. In a myelodysplastic/ myeloproliferative neoplasms (MDS/MPN) model, *Ptpn11* mutation in MSCs hyperactivates HSC by secreting CCL3, systemically resulting in myeloid-biased proliferation and promoting leukemia progression[5]. Chromosomal abnormalities in MSCs occur in over 16% MDS/acute myeloid leukemia (AML) patients, which leads to a shorter survival[6]. MSCs of every MDS patient show features of stemness loss, ageing, and osteogenic differentiation defect, which results in insufficient hematopoiesis[7]. In a patient-derived xenograft (PDX) model, only co-transplantation of tumor cells and the same patient-derived MSCs successfully recapitulates the MDS phenotype, indicating that besides the loss of function of supporting hematopoiesis, MSCs in MDS patients may acquire a function of preferentially promoting tumorigenesis[8]. Despite these findings, the causal relationship between tumor cells and the BM microenvironment during leukemia development and progression remains elusive.

MSC therapy has been widely used in treating immune-related graft-vs-host disease (GVHD) and inflammation-related diseases[9,10]. Over the decades, a lot of evidence demonstrate that MSCs regulate innate and adaptive immune responses largely by secreting distinct sets of cytokines, growth factors and chemokines depending on different disease contexts[11-15]. Given the short

lifespan of donor MSCs after transfusion[16], the underlying molecular and cellular mechanisms by which these cells produce therapeutic effects remain elusive. It is also completely unknown whether donor MSCs can restore the impaired BM microenvironment and consequently suppress disease progression in leukemia setting.

Macrophages are pivotal for maintenance of the tissue microenvironment, tissue repair and even the tumor microenvironment[17-21]. BM resident macrophages maintain the homeostasis of HSCs and loss of these macrophages leads to mobilization of HSCs into peripheral blood (PB)[22]. The functions of macrophages are plastic and can be reshaped by distinct sets of soluble factors. When performing tissue repair, macrophages highly express arginase 1 (*Arg1*)[23], an enzyme that converts L-arginine to urea and L-ornithine. After co-culture with MSCs, macrophages can be polarized from pro-inflammation (M1) to anti-inflammation (M2) type, up-regulating IL-10 and CD206 and down-regulating IL-6 and IL-1β[24]. Upon stimulated by LPS or TNF-α, MSCs can cross-talk with lung macrophages and reprogram these macrophages to secret IL-10 to alleviate sepsis[25]. Despite these knowledge, whether healthy MSCs can reprogram macrophages from leukemia-bearing host to repair the damaged BM microenvironment is not known.

Using the established mouse model mimicking chronic MPN/MDS diseases[18,26-28], we discovered that the deteriorating BM microenvironment was associated with disease progression. Intra-BM instead of systemic transfusion of healthy MSCs restored the local BM microenvironment, improved thrombopoiesis, reduced tumor burden, and prolonged survival of leukemia-bearing mice. Mechanistically, we found that MSCs suppress leukemia development through resident macrophages and autocrine effect of IL-6. Our study demonstrates that intra-BM transfusion of MSCs can restore the local BM niche to systemically prevent leukemia progression and can be a novel therapy for leukemia.

Results

Deterioration of BM MSCs accompanies the development of *Nras*-mutant-induced leukemia

Mice carrying an endogenous mutant *Nras* allele develop myelodysplastic/myeloproliferative neoplasms (MDS/MPN)-like leukemia with a long latency[18,26-28]. Here we found the primary BM leukemia cells failed to accelerate the disease in the secondary recipient mice, implying a role of the BM microenvironment in disease etiology (Fig. S1). We hypothesized that the BM microenvironment is impaired by *Nras*-mutant leukemia cells, which in return impedes normal hematopoiesis and accelerates leukemia progression. Indeed, we observed quantitative decreases and functional degeneration of MSCs ($Ter119^-CD45^-CD31^-Sca1^+CD51^+CD146^+$) during disease development and progression (Fig. 1a-c). To further characterize the residual MSCs in mice with leukemia, we performed RNA-Seq analysis of the residual MSCs from leukemia-bearing mice at an early disease phase ($CD11b^+$% in PB: 35%-45%). Consistent with the quantitative and functional reduction, the expression of the transcription factor *Gnl3*[29], an indicator of MSC self-renewal, was significantly down-regulated in MSCs from leukemia-bearing mice relative to wild-type mice (Fig. 1d). The expression of *Nt5e* (CD73)*, Thy1* (CD90), *Vcam1* (CD106)*, Cd81*, *Sdc4, Itgb1* and *Anpep*[29-31], encoding surface markers on three-lineage-potent MSCs but not on uni-lineage-primed MSCs, was markedly reduced in MSCs from leukemia-containing mice (padj < 0.05, fold change > 1.6) (Fig. 1d). Furthermore, the expression of *Bgn*, *Bmp4*, *Col1a1*, *Csf1*, *Dcn*, *Dkk2*, *Mmp13*, *Ogn*, *Wisp1*, and *Wisp2*[29,32], pivotal for osteogenic differentiation, was markedly suppressed in the residual MSCs (padj < 0.05, fold change > 2) (Fig. 1e). MSCs fulfill their tissue-specific and condition-responsive regulatory functions through secreting distinct types of soluble factors[33]. Under leukemia condition, the residual MSCs indeed secreted much less soluble factors, including *Il6, Il11, Ccl2, Ccl7, Cxcl12, Cxcl13* and *Cxcl14* (padj < 0.05, fold change > 2),

compared to MSCs from normal wild-type mice (Fig. 1f). These molecules are pivotal for tissue repairing[34-39]. In addition, *Ccl5,* a chemokine involved in the pathogenesis of MPN[40] and the inhibition of thrombopoiesis[41], was significantly up-regulated in the residual MSCs from leukemia-containing mice (padj < 0.05, fold change > 2). Gene set enrichment analysis (GSEA) further revealed features of inflammation in the residual MSCs (Fig. 1g). Collectively, these results show that the MSCs dramatically deteriorate during the disease development and progression of *Nras*-mutation-caused leukemia.

Intra-BM transfusion of healthy MSCs improves thrombopoiesis, reduces tumor burden and improves survival of the leukemia-bearing mice

We hypothesized that restoration of the impaired BM microenvironment in leukemia-bearing mice might suppress/delay the disease progression. To test this hypothesis, we attempted healthy MSC treatment using GFP-tagged MSCs isolated from the tibias and femurs of healthy mice as previously reported[42]. The isolated primary MSCs were expanded shortly *in vitro* to passage two (P2) and cryopreserved. For MSC treatment, the cryopreserved P2 MSCs were recovered and cultured for five days, phenotypically identified ($CD45^-Ter119^-CD31^-CD51^+CD105^+LepR^+PDGFR\alpha^+PDGFR\beta^+Sca1^+$) (Fig. S2), and suspended in DPBS (2.5 × 10^7/ml) for transfusion. Initially, we adopted a direct delivery procedure by injecting donor MSCs every two weeks either via tail vein (dose: 0.5 × 10^6/mouse) (Fig. S3a) or retro-orbital (dose: 0.5 × 10^6/mouse) transfusion (Fig. S3b) into the leukemia-bearing mice at a late disease phase ($CD11b^+$ cells > 60% in PB). However, these delivery approaches failed to produce therapeutic effects. *In vitro* cultured MSCs lose their natural homing feature[43]. Thus, we attempted intra-BM transfusion to overcome the homing defect caused by *in vitro* culture. A 2.5 × 10^7 MSCs/kg dose in 20 μL DPBS was injected into the tibia cavities of leukemia-bearing mice with

two-week intervals for up to 16 weeks (Fig. 2a). Strikingly, the tumor burden continuously decreased during MSC treatment (Fig. 2b). Consequently, the survival of treated leukemia-bearing mice was significantly prolonged (Untreated: 261.5 days, MSC-treated: >360 days, $p < 0.001$) (Fig. 2c). Therefore, intra-BM transfusion of healthy donor MSCs improves the survival of leukemia-bearing mice.

MSC-treatment systemically re-balances myelopoiesis and activates megakaryopoiesis

We next investigated the underlying mechanisms associated with the systemically decreased tumor burden. We found that the hematopoiesis in the MSC-treated leukemia-bearing mice was re-balanced, demonstrated by significant decreases of white blood cells (Untreated vs MSC-treated: 23.04 vs 8.876, $p = 0.009$), and significant elevation of platelets (Untreated vs MSC-treated: 2.64 vs 6.01, $p = 0.004$) (Fig. 2d) in PB. On the contrary, the PBS-treated leukemia-bearing mice exhibited neither improved hematopoiesis nor prolonged survivals (Fig. S4). High GM-CSF levels in serum are associated with the tumor burdens of CMML in patients[44] and mouse models[26]. We analyzed the GM-CSF levels in serum of leukemia-bearing mice with or without MSC-treatment. As expected, the GM-CSF levels in MSC-treated leukemia-bearing mice were significantly decreased (> 7 folds) ($p < 0.001$) (Fig. 2e). IL-6 promotes thrombopoiesis by increasing systemic TPO levels[45]. Consistently, the MSC-treated leukemia-bearing mice exhibited elevated IL-6 (> 25 folds) and TPO (> 2 folds) levels (Fig. 2f) in PB serum. Collectively, these results indicate that intra-BM transfusion of healthy donor MSCs systemically improves hematopoiesis and prolongs the survival of leukemia-bearing mice.

To further investigate the systemic effects of the local MSC-treatment on hematopoiesis in leukemia-bearing mice, we analyzed the ratios of myeloid progenitor subpopulations in MSC-treated leukemia-bearing mice. Consistent with the elevated platelet levels and reduced myeloid

cells in PB, the MSC-treated leukemia-bearing mice showed increased proportions of megakaryocyte-erythroid progenitors (MEP) (> 1.6 folds) ($p < 0.001$) and decreased ratios of granulocyte-macrophage progenitors (GMP) (> 1.5 folds) ($p < 0.001$) in both injected and non-injected sites than those sites in PBS-treated leukemia-bearing mice (Fig. 3a-b). In addition, we observed increased (> 1.3 folds) ratios of mature megakaryocytes (≥ 8N) in both injected and non-injected sites in MSC-treated leukemia-bearing mice (Fig. 3c-d) in comparison with PBS-treated leukemia-bearing control mice ($p < 0.001$). Thus, these data demonstrate that MSC-treatment systemically re-balances myelopoiesis and activates megakaryopoiesis in leukemia-bearing mice.

Recovered host MSCs are functional as healthy counterparts

To investigate whether the improved hematopoiesis is associated with restoration of the BM microenvironment, we analyzed the MSC-treated tibias eight weeks after MSC treatment. Interestingly, host MSC (GFP negative) were partially recovered (Fig. 4a-b), but restricted to the locally treated tibias (Fig. S5). Functionally, the recovered host MSCs formed markedly more CFU-F colonies than the residual MSCs from untreated leukemia-bearing mice (> 3.8 folds) ($p < 0.001$) (Fig. 4c and Fig. S6). To characterize the recovered MSCs at the transcriptome level, we sorted the recovered MSCs for RNA-Seq analysis. The expression of chemokines, including *Ccl2, Ccl7, Ccl19, Cxcl12, Cxcl13,* and *Cxcl14*, was restored in the recovered MSCs compared to that in MSCs from untreated leukemia-bearing control mice (padj < 0.05, fold change > 2) ($p < 0.05$) (Fig. 4d and Fig. S7). Unsupervised hierarchical clustering analysis showed that the recovered MSCs clustered closer to healthy MSCs (Fig. 4e). Therefore, donor MSC-treatment results in local functional restoration of host MSCs.

The donor MSCs reprogram macrophages to execute tissue-repair function

We further investigated the cellular mechanism underlying the restored BM microenvironment mediated by donor MSCs under leukemia condition. BM macrophages play a pivotal role in maintaining the BM niche[17]. To study whether donor MSCs reprogram BM macrophages, we performed co-culture assay of healthy MSCs with BM macrophages (L-Mac) sorted from the leukemia-bearing mice *in vitro* for twelve hours and re-sorted the macrophages (E-Mac) for RNA-Seq analysis. GSEA illustrated that angiogenesis-related genes, including *Vegfa, Hif1a, Serpine1, Eng and Thbs1*[46] (Fig. S8a), were enriched among the differentially expressed genes in E-Mac (Fig. 5a). Genes associated with cell migration, including *Sirpa* and *Ccl5*[47,48], were also enriched in E-Mac (Fig. 5b and Fig. S8b). Further, gene-ontology analysis demonstrated features of positive regulation of cell migration and angiogenesis in E-Mac (Fig. 5c). An elevated expression of genes encoding soluble factors involving in tissue repairing[49,50], including *Ccr2*, *Ccl3*, *Ccl5* and *Il6*, was also observed in E-Mac (Fig. 5d). RNA-Seq analysis showed that the expression of arginase 1 (*Arg1*), an indicator of tissue repair function[23], was dramatically up-regulated over thousand folds in E-Mac (Fig. 5e) after direct co-culture with MSCs *in vitro*. However, the *Arg1* expression in macrophages after transwell co-culture was barely elevated (Fig. 5e), indicating that direct cell-cell interaction instead of MSC-secreted soluble factors is essential for the functional reprogramming. Consistent with the observation *in vitro*, the expression of *Arg1* was also significantly increased in BM macrophages directly isolated from MSC-treated leukemia-bearing mice (Fig. 5f). Collectively, these results indicate that the donor MSCs reprogram BM macrophages from leukemia-bearing mice to executing tissue-repair function.

The E-Mac treatment largely recapitulates the therapeutic effects of MSC treatment

Given the short lifespan of donor MSCs *in vivo*[16], we speculated that MSCs mediate the restoration of the BM microenvironment of leukemia-bearing mice by reprogramming macrophages. We

isolated macrophages from leukemia-bearing mice and co-cultured them with healthy MSCs for 12h, and then transplanted these E-Mac back into leukemia-bearing mice by intra-BM injection (Fig. 6a). We indeed found that the thrombopoiesis was significantly improved (> 6 folds) after E-Mac treatment ($p < 0.001$) (Fig. 6b-c). Host MSCs were also significantly increased (> 3 folds) in E-Mac-treated leukemia-bearing mice ($p < 0.001$) (Fig. 6d-e). Consistent with the MSC treatment, we also observed increased ratios of mature megakaryocytes ($p < 0.001$) (Fig. 6f-g) and alleviated tumor burden ($CD11b^+$) (Fig. S9) in E-Mac-treated leukemia-bearing mice. Collectively, these results demonstrate that MSC-reprogrammed macrophages largely recapitulate the therapeutic effects of MSCs.

MSCs reprogram macrophages and reduce leukemia burden through IL-6

Residual MSCs in leukemia-bearing mice lost abilities to secret IL-6 (Fig. 1f). IL-6 is critical for maintaining the stemness and function of MSCs[51]. The recovered host MSCs after donor MSC-treatment expressed comparable *Il6* mRNA as healthy MSCs (Fig. 4d). Consistently, BM plasma IL-6 levels in MSC-treated leukemia-bearing mice were significantly elevated (> 3 folds) and were comparable to those in healthy mice ($p < 0.001$) (Fig. 7a). To investigate the role of IL-6 in MSC-mediated therapeutic effects, we directly injected IL-6 proteins (40 μg/kg) into leukemia-bearing mice. However, systemic IL-6 transfusion failed to suppress leukemia (Fig. S10). We speculated that IL-6 might function as an autocrine factor for MSCs to reprogram macrophages in leukemia-bearing mice. *In vitro* co-culture assay showed that $Il6^{-/-}$ MSCs compromised their ability to induce *Arg1* expression in macrophages derived from leukemia-bearing mice (Fig. 7b). In addition, intra-BM injection of $Il6^{-/-}$ MSCs neither improved thrombopoiesis nor reduced tumor burden in leukemia-bearing mice (Fig. 7c-e). Furthermore, $Il6^{-/-}$ MSCs failed to reprogram macrophages in leukemia-bearing mice *in vivo* (Fig. 7f). Taken together, these results demonstrate that autocrine

IL-6 is essential for MSC-mediated reprogramming of macrophages and reduction of tumor burden in leukemia-bearing mice.

Discussion

Deteriorating BM microenvironment accompanies chronic leukemia progression. Here we unravel a *de novo* approach of reverting the impaired BM microenvironment by intra-BM injection of donor MSCs. Upon injection, the donor MSCs quickly reprogrammed local host BM macrophages to repair the niche, thus improving normal hematopoiesis and suppressing leukemia development. These effects of donor MSCs depend on the autocrine production of IL-6. Our studies reveal de novo mechanisms underlying MSC-mediated local BM microenvironment restoration that systemically suppress leukemia development.

Given the short-term lifespan of the exogenous MSC *in vivo*, it is surprising that local injection of donor MSCs results in long-term improvement of thrombopoiesis and reduction of tumor burden. Following injection, exogenous donor MSCs immediately reprogram host resident macrophages that further organize the overhaul of local BM microenvironment, including restoring the functions of host MSCs. There are a lot of evidence supporting the pivotal roles of macrophages in tissue repair[49,52]. Donor MSCs can transiently release a key wave of tissue-repair factors, such as IL-6[34], CCL7[39] and CXCL12[36], and reprogram host macrophages, subsequently resulting in the recovery of host MSCs. Recovered host MSCs further secreted much higher level of CCL2, CCL7 and CXCL12 that can further facilitate BM niche repair. Donor MSCs could also directly modulate the other niche cells, in addition to macrophages, to participate in BM niche repair[11]. Consequently, the restored local BM microenvironment outputs abundant hematopoiesis-improving cytokines, including IL-6[45], and reduces tumor-growth-stimulating cytokines, such as GM-CSF[26,44]. Thus,

despite the short life-span, donor MSCs provide long-term thrombopoiesis improvement and tumor burden reduction through the stepwise microenvironment restoration.

Of note, IL-6 deficiency in MSCs markedly compromised the abilities of these cells to reprogram host resident macrophage. Transwell co-culture study has shown that direct interaction between MSCs and macrophages is required for reprogramming host macrophages. Both autocrine production of IL-6 and reprogramming host macrophages by MSCs are required for MSC-mediated microenvironment restoration and leukemia inhibition. However, it is not clear how autocrine IL-6 controls the function of MSCs and how MSCs directly reprogram macrophages. The underlying molecular mechanisms warrant further investigation.

MSC treatment inhibits leukemia development in the *Nras*-mutation-induced MPN/MDS-like disease model. We also attempted to broaden MSC treatment for acute leukemia in the MLL-AF9-initiated model (Fig. S11a), in which impaired MSCs results in the reduction of osteogenesis and CXCL12 production[53]. Despite a mild elevation of platelet level, the intra-BM transfusion of donor MSCs failed to significantly improve normal hematopoiesis or suppress acute leukemia development (Fig. S11b-h). Therefore, the intra-BM MSC treatment might be beneficial for MPN/MDS leukemias, such as JMML and CMML, but insufficient for suppressing acute leukemia. Although MSC application could be an effective therapeutic regimen for patients with MPN/MDS-subtype leukemia, combination therapy of conventional approaches with local MSC transfusion might be required to achieve therapeutic outcomes for acute leukemia with impaired BM microenvironment.

Methods

Mice. All mouse strains were maintained on C57BL/6 genetic background. Mice expressing the conditional oncogenic NrasG12D mutation (a gift from Dr. Jing Zhang lab at University of

Wisconsin-Madison, Wisconsin, USA) were crossed to Vav-Cre mice to generate *LSL Nras*/+; *Vav-Cre* compound mice (NV mice). Genotyping of the adult mice was performed as described previously[26]. Vav-Cre strain (CD45.2), wild-type CD45.2, CD45.1 strain (C57BL/6) and *Il6* knock out strain (*Il6*$^{-/-}$, C57BL/6) were purchased from Jackson lab. GFP strain (CD45.2) was gifted by Guangdong Laboratory Animals Monitoring Institute. *MLL-AF9* AML model mice were maintained a specific pathogen-free animal facility at the State Key Laboratory of Experimental Hematology. All mice were maintained within the SPF grade animal facility of Guangzhou Institution of Biomedicine and Health, Chinese Academy of Science (GIBH, CAS, China). All animal experiments were approved by the Institutional Animal Care and Use Committee of Guangzhou Institutes of Biomedicine and Health (IACUC-GIBH).

NrasG12D leukemia model. White blood cells (CD45.2^{+}, 0.3 million) after depletion of stromal cells from NrasG12D compound mice (*LSL Nras/+; Vav-Cre*) or control mice (CD45.2 strain) were sorted and transplanted into sublethally (6.5 Gy, RS2000, Rad Source Inc) irradiated CD45.1 recipient by retro-orbital intravenous injection. Mice were fed with trimethoprim-sulfamethoxazole-treated water for two weeks to prevent infection. Hematopoietic lineages in PB were assessed monthly by flow cytometry. During the development of NrasG12D-induced leukemia, the CD11b^{+} percentage in PB indicated the tumor burden (CD11b^{+}%).

MLL-AF9 AML mouse model. We used a non-irradiated acute myeloid leukemia mouse model described previously[54].

Flow cytometry analysis. Antibodies for hematopoietic lineage analysis: FITC-TER-119 (TER-119), PerCP-Cyanine5.5-CD45.2 (104), APC-Thy1.2 (53-2.1), APC-CD3e (145-2C11), PE-CD19 (1D3), PE-Cy7-CD11b (M1/70), APC-eFluor®780-Gr-1 (RB6-8C5), FITC-CD41 (MWReg30),

PE-CD61 (2C9.G3) and APC-eFluor®780-F4/80 (BM8) antibodies were purchased from eBiosciences. DAPI was used to exclude dead cells.

For MSC analysis, BMNC were stained with the following antibodies: APC-Ter119 (TER-119), APC-CD45 (30-F11), PE-Cy7-CD31 (WM-59), APC-eFluor®780-Sca1 (D7), PE-CD51 (RMV-7), and PerCP-Cyanine5.5-CD146 (ME-9F1) were purchased from eBiosciences or Biolegend. DAPI was used to exclude dead cells.

For myeloid progenitors staining, BM cells were stained with the following antibodies: CD2 (RM2-5), CD3e (145-2C11), CD4 (RM4-5), CD8a (53-6.7), Ter119 (TER-119), CD11b (M1/70), B220 (6B2), Gr1 (RB6-8C5), IL-7R (A7R34), Sca1 (E13-161.7), c-kit (2B8), CD34 (RAM34), and CD16/32 (93). DAPI was used to exclude dead cells.

For megakaryocyte maturation detection, BM cells were stained with labeled with CD41-FITC (MWReg30). Then cells were fixed using cold 70% ethanol. After washing, the fixed cells were resuspended in propidium iodide.

For platelet staining and counting, 5 μL fresh whole blood was collected. Whole blood sample was blocked with anti-mouse CD16/32, then was stained with anti-mouse CD41-FITC and anti-mouse CD61-PE at room temperature for 20 mins. Then 1 mL of cold 1% PFA solution and 50 μL absolute counting beads (C36950, Invitrogen) were added to each sample. The sample was fixed on ice for at least 30 mins.

The stained cells were analyzed on LSR Fortessa (BD Bioscience), then the data were analyzed using Flowjo software (FlowJo).

Preparation of BMNC. Mice were sacrificed, and BM cells were isolated by flushing out the tibias and femurs using DPBS containing 2% FBS. The compact bones were dissected into ~2 mm fragments and transferred with 5ml of 1 mg/ml collagenase II solution into a 50 ml tube. The tubes

were incubated in a shaker (< 110 rpm) at 37°C for 1-2 hours. BMNC from BM cells and compact bones were mixed and filtered through a 70 μm cell strainer (BD Falcon) to obtain a single-cell suspension.

MSC sorting. BMNC mixtures of BM and compact bones from the control mice (age-matched wild-type, $CD11b^+$% in PB = 10-15%), leukemia-bearing mice ($CD11b^+$% in PB = 35%-45%) and leukemia-bearing mice eight weeks post-treatment with GFP^+ MSCs were isolated as previously described. After lysis of red blood cells, BMNC were blocked by Fc blocker, and incubated with biotin-conjugated anti-CD45 antibody and enriched by streptavidin magnetic beads (Miltenyi Bitec). The enriched $CD45^-$ cells were stained with the following antibodies: APC-Ter119 (TER-119), APC-CD45 (30-F11), streptavidin-APC, PE-Cy7-CD31 (WM-59), APC-eFluor®780-Sca1 (D7), PE-CD51 (RMV-7) were purchased from eBiosciences. DAPI was used to exclude dead cells. MSCs were sorted by the gating strategy defining as $GFP^-Ter119^-CD45^-CD31^-Sca1^+CD51^+$ using AriaII (BD Bioscience) and subsequently prepared for RNA-Seq.

Mouse colony-forming unit-fibroblast (CFU-F) assay. For analyzing the quantity of functional MSCs, BMNC equivalent to 100 MSCs from each mouse were used as cell input for individual wells (six-well plate). BMNC were suspended into 2 ml of mouse complete MesenCult™ medium (Catalog 05513, StemCell Technology), then seeded into the individual wells. BMNC were incubated at 37°C with 5% CO_2 in a humidified chamber. Half-medium change was performed on day 7. After 14 days, the wells were washed once with DPBS and fixed by ice-cold ethanol, and then stained with giemsa stain at RT. After washing, colonies with more than 20 spindle-shaped cells per colony were counted. Three replicates of each sample were performed.

Isolation and expansion of mouse MSCs. MSCs were isolated from cell mixture of compact bones and BM cells of 3-4 weeks old healthy GFP mice (n = 100) or *Il6*$^{-/-}$ mice, as previously

reported with minor modifications[42]. Briefly, the BM cavities were flushed in order to thoroughly deplete hematopoietic cells. The compact bones were dissected into ~2 mm fragments and transferred with 5ml of 1 mg/ml collagenase II solution into a 50 ml tube. The tubes were incubated in a shaker (< 110 rpm) at 37^{o}C for 1-2 hours. The fragments were washed three times and cultivated in complete MSC culture medium (α-MEM (Gibco) supplemented with 10% FBS (Gibco) and 1% penicillin/streptomycin (Invitrogen)) in a 6 cm dish. Besides, MSCs from the BM cells were sorted (Ter119^{-}CD45^{-}CD31^{-}Sca1^{+}CD51^{+}CD146^{+}) directly into MSC culture medium. These two sources of MSCs from compact bones and BM cells were mixed for further isolation and expansion. The bone fragments were removed, and culture medium was replaced after three times' washing on the third day. After culture for five days, the adherent cells were harvested by 0.25% trypsin's digestion and passaged. The culture medium was changed every 48 hours and passaged at a split ratio of 1:3 every 3-4 days. The expanded MSCs (Passage 2) were cryopreserved with 90% DMSO and 10% FBS in liquid nitrogen for transfusion. The cryopreserved P2 MSCs were recovered and cultured for 4-5 days, phenotypically identified, and collected in DPBS (2.5 × 10^7/ml) for transfusion.

RNA-Seq and data analysis. For MSC library preparation, MSCs were sorted from wild type or leukemia-bearing mice, and recovered MSC were sorted from leukemia-bearing mice 8 weeks post treatment with GFP^{+} donor MSCs. MSCs were sorted from two mice of each group. 1000 target cells per sample were sorted into 500 μl DPBS-BSA buffer (0.5%BSA) using 1.5ml EP tube and transferred into 250 μl tube to spin down with 500 g. The cDNA of sorted 1000-cell aliquots were generated and amplified as described previously[55]. The qualities of the amplified cDNA were examined by Q-PCR analysis of housekeeping genes (*B2m, Actb, Gapdh, Ecf1a1*). Samples passed

363 quality control were used for sequencing library preparation by illumina Nextera XT DNA Sample
364 Preparation Kit (FC-131-1096).
365 For macrophages (*in vivo*) library preparation, macrophages were sorted from BM of leukemia-
366 bearing mice before or after MSC treatment (12 hours post MSC treatment). Macrophages were
367 also sorted after 12 hours of co-culture with MSCs. 1 × 10^5 target cells per sample were sorted,
368 and total RNA was extracted using the RNeasy micro kit with on-column DNase treatment
369 (Qiagen, 74004) according to manufacture's protocol. cDNA library was constructed using
370 VAHTSTM mRNA-seq V3 Library Prep Kit for Illumina (Vazyme, NR611) according to
371 manufacture's protocol. The qualities of the cDNA were examined by qPCR analysis of
372 housekeeping genes (*B2m, Actb, Gapdh, Ecf1a1*). Samples that passed quality control were used
373 for sequencing.
374 For data analysis, all libraries were sequenced by illumina sequencers NextSeq 500. The fastq files
375 of sequencing raw data samples were generated using illumina bcl2fastq software (version:
376 2.16.0.10) and were uploaded to Gene Expression Omnibus public database (GSE 125029). Raw
377 reads were aligned to mouse genome (mm10) by HISAT2[56] (version: 2.1.0) as reported. And raw
378 counts were calculated by featureCounts of subread[57] (version 1.6.0). Differential gene expression
379 analysis was performed by DESeq2[58] (R package version: 1.18.1). Unsupervised clustering
380 analysis was performed using facotextra (R package, version： 1.0.5). Heatmaps were plotted
381 using gplots (R package, version 3.01). GSEA was performed as described[59], and gene-ontology
382 (GO)-enrichment analysis were performed by clusterProfiler[60] (R package, version: 3.6.0). MSC
383 stemness related genes and MSC osteogenesis related genes for heatmaps were from literatures as
384 follows: MSC stemness-related genes[29-31] and MSC osteogenesis-related genes[29,32]. The gene sets
385 for GSEA were from literatures as follows: angiogenesis related genes in macrophages[46], cell

migration related genes in macrophages (from MSigDB genesets), and secreted factors by macrophages[61,62].

MSC treatment for leukemia-bearing mice. For MSC transfusion, multiple approaches including retro-orbital, tail intravenous and local intra-BM transfusion were applied independently. For tail vein transfusion, each leukemia-bearing mouse was injected with 2.5 × 10^7 MSCs/kg (Passage 2) in 100 μl DPBS by tail vein transfusion. For retro-orbital transfusion, each leukemia-bearing mouse was injected with 2.5 × 10^7 MSCs/kg (Passage 2) in 200 μl DPBS by retro-orbital transfusion. For local intra-BM transfusion, tibia of each leukemia-bearing mouse was injected with 2.5 × 10^7 MSCs/kg (Passage 2) in 20 μl DPBS by local intra-BM transfusion. MSCs were injected once every two weeks and continued in a time window of 16 weeks. Every tibia was treated once per month by switching the injection site every other dose. The control mice were injected with DPBS following the same treatment procedure as MSCs. Analysis of platelets and $CD11b^+$ cells in PB was performed monthly.

GFP-MSC and BM macrophage co-culture assay. Short-term co-culture assay was performed, with each well containing: 1 × 10^5 GFP-MSCs (passage 2; healthy MSCs were isolated from GFP mice, *Il6*$^{-/-}$ MSCs were isolated from *Il6*$^{-/-}$ mice) and 2 × 10^6 $CD11b^+$ leukemia cells sorted from leukemia-bearing mice in 2 mL culture medium of α-MEM, 10% FBS and 50 ng/ml SCF. MSCs and $CD11b^+$ leukemia cells were incubated either by direct-contact culture or transwell culture for 12 hours at 37°C under 5% CO_2 in a humidified incubator. MSC-reprogrammed macrophages from leukemia-bearing mice ($CD11b^+F4/80^+$) were sorted for detecting the gene expression by Q-PCR.

Treatment for leukemia-bearing mice with MSC-reprogrammed macrophages. 1 × 10^5 MSCs were seeded into each well of six-well plates. $CD11b^+$ leukemia cells were enriched from

BM of leukemia-bearing mice with severe tumor burden ($CD11b^+$% in PB > 60%). Then 2 × 10^6 $CD11b^+$ leukemia cells were directly co-cultured with MSCs. After 12 hours, macrophages were sorted for transfusion. Leukemia-bearing mice with severe tumor burden were treated by intra-BM transfusion of PBS or MSC-reprogrammed macrophages from leukemia-bearing mice (E-Mac). A dose of 1 million macrophages/mouse in 20 μl PBS were delivered into the tibia cavity using 29-gauge needle. Every tibia was treated once per two weeks by switching the injection site every other dose. Analysis of platelets and $CD11b^+$ cells in PB was performed monthly.

Complete blood count (CBC). For mouse samples, 100 μl PB from each mouse was collected into 1.5 ml anticoagulation tube and diluted with the same volume of PBS, then performed complete blood count by automatic blood analyzer (Abbott, CD3700SL).

Enzyme-linked immunosorbent assay (ELISA) assay. For mouse samples, serum was collected from PB of control mice and leukemia-bearing mice; and BM plasma samples were collected from tibias and femurs of control mice and leukemia-bearing mice by flushing out the BM using 1-2 ml PBS. The supernatants were collected for ELISA after centrifugation. The concentration of cytokines, mouse IL-6 (CME0006-96) and mouse GM-CSF (CME0026-96), were measured using ELISA kits (Beijing 4A Biotech Corporation, China) according to the manufacture's instruction. The concentration of cytokine, mouse TPO (BEK-2096-1P), was measured using ELISA kits (Biosensis) according to the manufacture's instruction.

mIL-6 treatment for leukemia-bearing mice. A dose of 40 μg/kg mIL-6 was injected into each leukemia-bearing mouse by intraperitoneal injection. mIL-6 was injected once every day and continued in a time window of 4 weeks. Analysis of tumor burden ($CD11b^+$ cells) in PB was performed every two weeks.

Quantitative real-time PCR. For analysis of mRNA expression levels of related genes in MSCs and $CD11b^+$ leukemia cells from the co-culture assay, 1 × 10^5 target cells of each sample were sorted by flow cytometry using Aria II. Total RNA was extracted using the RNeasy Micro Kit (Cat NO. 74004, QIAGEN). On-column DNase digestion of the samples was performed following manufacturer's instruction. First strand cDNA was synthesized from 100 ng of total RNA in 20 μl final volume, using the ReverTra Ace qPCR RT Master Mix kit (FSQ-301, TOYOBO) according to the manufacturer's instructions. Real-time quantitative PCR assays were carried out in a BioRad CFX96 Real-Time PCR Detection System instrument (Bio-Rad) using standard PCR conditions. Triplicates of all reactions were performed. GAPDH gene was used as a reference for differential expression comparison. The primer sequences of all related genes are shown in Table S1.

Statistical analysis. The data were represented as mean ± SD. Two-tailed independent Student's t-tests were performed for comparison of two groups of data (SPSS v.23, IBM Corp., Armonk, NY, USA). For the analysis of three groups or more, one-way ANOVA was used (SPSS v.23, IBM Corp., Armonk, NY, USA), and further significance analysis among groups was analyzed by Post Hoc Test (equal variances, Turkey-HSD; unequal variances, Games-Howell). Kaplan-Meier method was used to calculate survival curves of leukemia, and Log-rank (Mantel-Cox) test was performed to compare differential significance in survival rates. P values of less than 0.05 were considered statistically significant (*$p < 0.05$, **$p < 0.01$, ***$p < 0.001$).

Data availability: The data that support the findings of this study are available from the corresponding author upon reasonable request.

References

1 Kfoury, Y. & Scadden, D. T. Mesenchymal cell contributions to the stem cell niche. *Cell Stem Cell* **16**, 239-253, doi:10.1016/j.stem.2015.02.019 (2015).

2 Raaijmakers, M. H. *et al.* Bone progenitor dysfunction induces myelodysplasia and secondary leukaemia. *Nature* **464**, 852-857, doi:10.1038/nature08851 (2010).

3 Schepers, K. *et al.* Myeloproliferative neoplasia remodels the endosteal bone marrow niche into a self-reinforcing leukemic niche. *Cell Stem Cell* **13**, 285-299, doi:10.1016/j.stem.2013.06.009 (2013).

4 Bowers, M. *et al.* Osteoblast ablation reduces normal long-term hematopoietic stem cell self-renewal but accelerates leukemia development. *Blood* **125**, 2678-2688, doi:10.1182/blood-2014-06-582924 (2015).

5 Dong, L. *et al.* Leukaemogenic effects of Ptpn11 activating mutations in the stem cell microenvironment. *Nature* **539**, 304-308, doi:10.1038/nature20131 (2016).

6 Blau, O. *et al.* Mesenchymal stromal cells of myelodysplastic syndrome and acute myeloid leukemia patients have distinct genetic abnormalities compared with leukemic blasts. *Blood* **118**, 5583-5592, doi:10.1182/blood-2011-03-343467 (2011).

7 Pandis, N. *et al.* Complex chromosome rearrangements involving 12q14 in two uterine leiomyomas. *Cancer Genet Cytogenet* **49**, 51-56 (1990).

8 Medyouf, H. *et al.* Myelodysplastic cells in patients reprogram mesenchymal stromal cells to establish a transplantable stem cell niche disease unit. *Cell Stem Cell* **14**, 824-837, doi:10.1016/j.stem.2014.02.014 (2014).

9 Ren, G. *et al.* Mesenchymal stem cell-mediated immunosuppression occurs via concerted action of chemokines and nitric oxide. *Cell Stem Cell* **2**, 141-150, doi:10.1016/j.stem.2007.11.014 (2008).

476 10 Prockop, D. J. Inflammation, fibrosis, and modulation of the process by mesenchymal
477 stem/stromal cells. *Matrix Biol* **51**, 7-13, doi:10.1016/j.matbio.2016.01.010 (2016).
478 11 Shi, Y. *et al.* Immunoregulatory mechanisms of mesenchymal stem and stromal cells in
479 inflammatory diseases. *Nat Rev Nephrol* **14**, 493-507, doi:10.1038/s41581-018-0023-5
480 (2018).
481 12 Le Blanc, K. & Mougiakakos, D. Multipotent mesenchymal stromal cells and the innate
482 immune system. *Nat Rev Immunol* **12**, 383-396, doi:10.1038/nri3209 (2012).
483 13 Mittal, M. *et al.* TNFalpha-stimulated gene-6 (TSG6) activates macrophage phenotype
484 transition to prevent inflammatory lung injury. *Proc Natl Acad Sci U S A* **113**, E8151-
485 E8158, doi:10.1073/pnas.1614935113 (2016).
486 14 Wang, G. *et al.* Kynurenic acid, an IDO metabolite, controls TSG-6-mediated
487 immunosuppression of human mesenchymal stem cells. *Cell Death Differ* **25**, 1209-1223,
488 doi:10.1038/s41418-017-0006-2 (2018).
489 15 Du, L. *et al.* IGF-2 Preprograms Maturing Macrophages to Acquire Oxidative
490 Phosphorylation-Dependent Anti-inflammatory Properties. *Cell Metab*,
491 doi:10.1016/j.cmet.2019.01.006 (2019).
492 16 Eggenhofer, E. *et al.* Mesenchymal stem cells are short-lived and do not migrate beyond
493 the lungs after intravenous infusion. *Front Immunol* **3**, 297,
494 doi:10.3389/fimmu.2012.00297 (2012).
495 17 Ehninger, A. & Trumpp, A. The bone marrow stem cell niche grows up: mesenchymal
496 stem cells and macrophages move in. *J Exp Med* **208**, 421-428, doi:10.1084/jem.20110132
497 (2011).

18 Chen, J. *et al.* CCL18 from tumor-associated macrophages promotes breast cancer metastasis via PITPNM3. *Cancer Cell* **19**, 541-555, doi:10.1016/j.ccr.2011.02.006 (2011).

19 Gubin, M. M. *et al.* High-Dimensional Analysis Delineates Myeloid and Lymphoid Compartment Remodeling during Successful Immune-Checkpoint Cancer Therapy. *Cell* **175**, 1014-1030 e1019, doi:10.1016/j.cell.2018.09.030 (2018).

20 Chen, C. C. *et al.* Organ-level quorum sensing directs regeneration in hair stem cell populations. *Cell* **161**, 277-290, doi:10.1016/j.cell.2015.02.016 (2015).

21 Liu, C. *et al.* Macrophages Mediate the Repair of Brain Vascular Rupture through Direct Physical Adhesion and Mechanical Traction. *Immunity* **44**, 1162-1176, doi:10.1016/j.immuni.2016.03.008 (2016).

22 Winkler, I. G. *et al.* Bone marrow macrophages maintain hematopoietic stem cell (HSC) niches and their depletion mobilizes HSCs. *Blood* **116**, 4815-4828, doi:10.1182/blood-2009-11-253534 (2010).

23 Bosurgi, L. *et al.* Macrophage function in tissue repair and remodeling requires IL-4 or IL-13 with apoptotic cells. *Science* **356**, 1072-1076, doi:10.1126/science.aai8132 (2017).

24 Cho, D. I. *et al.* Mesenchymal stem cells reciprocally regulate the M1/M2 balance in mouse bone marrow-derived macrophages. *Exp Mol Med* **46**, e70, doi:10.1038/emm.2013.135 (2014).

25 Nemeth, K. *et al.* Bone marrow stromal cells attenuate sepsis via prostaglandin E(2)-dependent reprogramming of host macrophages to increase their interleukin-10 production. *Nat Med* **15**, 42-49, doi:10.1038/nm.1905 (2009).

519 26 Wang, J. *et al.* Endogenous oncogenic Nras mutation promotes aberrant GM-CSF signaling
520 in granulocytic/monocytic precursors in a murine model of chronic myelomonocytic
521 leukemia. *Blood* **116**, 5991-6002, doi:10.1182/blood-2010-04-281527 (2010).
522 27 Wang, J. *et al.* Endogenous oncogenic Nras mutation initiates hematopoietic malignancies
523 in a dose- and cell type-dependent manner. *Blood* **118**, 368-379, doi:10.1182/blood-2010-
524 12-326058 (2011).
525 28 Wang, J. Y. *et al.* Nras(G12D/+) promotes leukemogenesis by aberrantly regulating
526 hematopoietic stem cell functions. *Blood* **121**, 5203-5207, doi:10.1182/blood-2012-12-
527 475863 (2013).
528 29 Freeman, B. T., Jung, J. P. & Ogle, B. M. Single-Cell RNA-Seq of Bone Marrow-Derived
529 Mesenchymal Stem Cells Reveals Unique Profiles of Lineage Priming. *PLoS One* **10**,
530 e0136199, doi:10.1371/journal.pone.0136199 (2015).
531 30 Song, L., Webb, N. E., Song, Y. & Tuan, R. S. Identification and functional analysis of
532 candidate genes regulating mesenchymal stem cell self-renewal and multipotency. *Stem*
533 *Cells* **24**, 1707-1718, doi:10.1634/stemcells.2005-0604 (2006).
534 31 Rostovskaya, M. & Anastassiadis, K. Differential expression of surface markers in mouse
535 bone marrow mesenchymal stromal cell subpopulations with distinct lineage commitment.
536 *PLoS One* **7**, e51221, doi:10.1371/journal.pone.0051221 (2012).
537 32 Delorme, B. *et al.* Specific lineage-priming of bone marrow mesenchymal stem cells
538 provides the molecular framework for their plasticity. *Stem Cells* **27**, 1142-1151,
539 doi:10.1002/stem.34 (2009).

33 Gnecchi, M., Danieli, P., Malpasso, G. & Ciuffreda, M. C. Paracrine Mechanisms of Mesenchymal Stem Cells in Tissue Repair. *Methods Mol Biol* **1416**, 123-146, doi:10.1007/978-1-4939-3584-0_7 (2016).

34 Gallucci, R. M. *et al.* Impaired cutaneous wound healing in interleukin-6-deficient and immunosuppressed mice. *FASEB J* **14**, 2525-2531, doi:10.1096/fj.00-0073com (2000).

35 Castela, M. *et al.* Ccl2/Ccr2 signalling recruits a distinct fetal microchimeric population that rescues delayed maternal wound healing. *Nat Commun* **8**, 15463, doi:10.1038/ncomms15463 (2017).

36 Kato, T. *et al.* SDF-1 improves wound healing ability of glucocorticoid-treated adipose tissue-derived mesenchymal stem cells. *Biochem Biophys Res Commun* **493**, 1010-1017, doi:10.1016/j.bbrc.2017.09.100 (2017).

37 Hayashi, Y. *et al.* CXCL14 and MCP1 are potent trophic factors associated with cell migration and angiogenesis leading to higher regenerative potential of dental pulp side population cells. *Stem Cell Res Ther* **6**, 111, doi:10.1186/s13287-015-0088-z (2015).

38 Sims, N. A. *et al.* Interleukin-11 receptor signaling is required for normal bone remodeling. *J Bone Miner Res* **20**, 1093-1102, doi:10.1359/JBMR.050209 (2005).

39 Schenk, S. *et al.* Monocyte chemotactic protein-3 is a myocardial mesenchymal stem cell homing factor. *Stem Cells* **25**, 245-251, doi:10.1634/stemcells.2006-0293 (2007).

40 Kleppe, M. *et al.* JAK-STAT pathway activation in malignant and nonmalignant cells contributes to MPN pathogenesis and therapeutic response. *Cancer Discov* **5**, 316-331, doi:10.1158/2159-8290.CD-14-0736 (2015).

41 Pang, L., Weiss, M. J. & Poncz, M. Megakaryocyte biology and related disorders. *J Clin Invest* **115**, 3332-3338, doi:10.1172/JCI26720 (2005).

42 Zhu, H. *et al.* A protocol for isolation and culture of mesenchymal stem cells from mouse compact bone. *Nat Protoc* **5**, 550-560, doi:10.1038/nprot.2009.238 (2010).

43 Rombouts, W. J. & Ploemacher, R. E. Primary murine MSC show highly efficient homing to the bone marrow but lose homing ability following culture. *Leukemia* **17**, 160-170, doi:10.1038/sj.leu.2402763 (2003).

44 Padron, E. *et al.* GM-CSF-dependent pSTAT5 sensitivity is a feature with therapeutic potential in chronic myelomonocytic leukemia. *Blood* **121**, 5068-5077, doi:10.1182/blood-2012-10-460170 (2013).

45 Kaser, A. *et al.* Interleukin-6 stimulates thrombopoiesis through thrombopoietin: role in inflammatory thrombocytosis. *Blood* **98**, 2720-2725 (2001).

46 Medina, R. J. *et al.* Myeloid angiogenic cells act as alternative M2 macrophages and modulate angiogenesis through interleukin-8. *Mol Med* **17**, 1045-1055, doi:10.2119/molmed.2011.00129 (2011).

47 Ohnishi, H. *et al.* Ectodomain shedding of SHPS-1 and its role in regulation of cell migration. *J Biol Chem* **279**, 27878-27887, doi:10.1074/jbc.M313085200 (2004).

48 Hocking, A. M. The Role of Chemokines in Mesenchymal Stem Cell Homing to Wounds. *Adv Wound Care (New Rochelle)* **4**, 623-630, doi:10.1089/wound.2014.0579 (2015).

49 Wynn, T. A. & Vannella, K. M. Macrophages in Tissue Repair, Regeneration, and Fibrosis. *Immunity* **44**, 450-462, doi:10.1016/j.immuni.2016.02.015 (2016).

50 Maurer, M. & von Stebut, E. Macrophage inflammatory protein-1. *Int J Biochem Cell Biol* **36**, 1882-1886, doi:10.1016/j.biocel.2003.10.019 (2004).

584 51 Pricola, K. L., Kuhn, N. Z., Haleem-Smith, H., Song, Y. & Tuan, R. S. Interleukin-6
585 maintains bone marrow-derived mesenchymal stem cell stemness by an ERK1/2-
586 dependent mechanism. *J Cell Biochem* **108**, 577-588, doi:10.1002/jcb.22289 (2009).
587 52 Liu, C. *et al.* Macrophages Mediate the Repair of Brain Vascular Rupture through Direct
588 Physical Adhesion and Mechanical Traction. *Immunity* **44**, 1162-1176,
589 doi:10.1016/j.immuni.2016.03.008 (2016).
590 53 Hanoun, M. *et al.* Acute myelogenous leukemia-induced sympathetic neuropathy promotes
591 malignancy in an altered hematopoietic stem cell niche. *Cell Stem Cell* **15**, 365-375,
592 doi:10.1016/j.stem.2014.06.020 (2014).
593 54 Cheng, H. *et al.* Leukemic marrow infiltration reveals a novel role for Egr3 as a potent
594 inhibitor of normal hematopoietic stem cell proliferation. *Blood* **126**, 1302-1313,
595 doi:10.1182/blood-2015-01-623645 (2015).
596 55 Tang, F. *et al.* RNA-Seq analysis to capture the transcriptome landscape of a single cell.
597 *Nat Protoc* **5**, 516-535, doi:10.1038/nprot.2009.236 (2010).
598 56 Kim, D., Langmead, B. & Salzberg, S. L. HISAT: a fast spliced aligner with low memory
599 requirements. *Nat Methods* **12**, 357-360, doi:10.1038/nmeth.3317 (2015).
600 57 Liao, Y., Smyth, G. K. & Shi, W. featureCounts: an efficient general purpose program for
601 assigning sequence reads to genomic features. *Bioinformatics* **30**, 923-930,
602 doi:10.1093/bioinformatics/btt656 (2014).
603 58 Love, M. I., Huber, W. & Anders, S. Moderated estimation of fold change and dispersion
604 for RNA-seq data with DESeq2. *Genome Biol* **15**, 550, doi:10.1186/s13059-014-0550-8
605 (2014).

606 59 Subramanian, A. *et al.* Gene set enrichment analysis: a knowledge-based approach for
607 interpreting genome-wide expression profiles. *Proc Natl Acad Sci U S A* **102**, 15545-
608 15550, doi:10.1073/pnas.0506580102 (2005).
609 60 Yu, G., Wang, L. G., Han, Y. & He, Q. Y. clusterProfiler: an R package for comparing
610 biological themes among gene clusters. *OMICS* **16**, 284-287, doi:10.1089/omi.2011.0118
611 (2012).
612 61 Arango Duque, G. & Descoteaux, A. Macrophage cytokines: involvement in immunity and
613 infectious diseases. *Front Immunol* **5**, 491, doi:10.3389/fimmu.2014.00491 (2014).
614 62 Cavaillon, J. M. Cytokines and macrophages. *Biomed Pharmacother* **48**, 445-453 (1994).
615

Acknowledgments

This work was supported by grants from the Strategic Priority Research Program of Chinese Academy of Sciences (XDA16010208), the Chinese Ministry of Science and Technology (2015CB964401, 2016YFA0100601, 2017YFA0103401, and 2015CB964902), the CAS Key Research Program of Frontier Sciences (QYZDB-SSW-SMC057), the Major Research and Development Project of Guangzhou Regenerative Medicine and Health Guangdong Laboratory (2018GZR110104006), the Health and Medical Care Collaborative Innovation Program of Guangzhou Scientific and Technology (201803040017), CAMS Innovation Fund for Medical Sciences (2016-12M-1-002), the Major Scientific and Technological Project of Guangdong Province (2014B020225005), co-operation Program from Guangdong Natural Science Foundation (2014A030312012), the General Program from Guangzhou Scientific and Technological Project (201707010157), the Science and Technology Planning Project of Guangdong Province (2017B030314056), the Program for Guangdong Introducing Innovative and Entrepreneurial Teams (2017ZT07S347), the grants from the National Natural Science Foundation of China (Grant No 31471117, 31271457, 81470281, 81421002, 81730006, and 3150094), the grants from the Ministry of Science and Technology of China (2016YFA0100600), and grants from NIH, USA (AI079087, D.W. and HL130724 D.W.)

Author Contributions

C.X.X. performed research, analyzed data and wrote the manuscript; D.Y. and Q.T.W. analyzed RNA-Seq data; T.J.W., H.C., P.Q.Z., K.T.W., X.F.L., Y.G., S.H.M., L.X. and Y.X.G. performed experiments; S.H., J.D., X.D., Y.Q.L., X.F.Z., Y.F.S. and S.X. discussed the manuscript; D.W. discussed the project and wrote the manuscript. T.C. and J.Y.W. designed the research and wrote the manuscript.

639 **Competing interest:** The authors declare no competing interests.

Figures and figure legends

Fig. 1

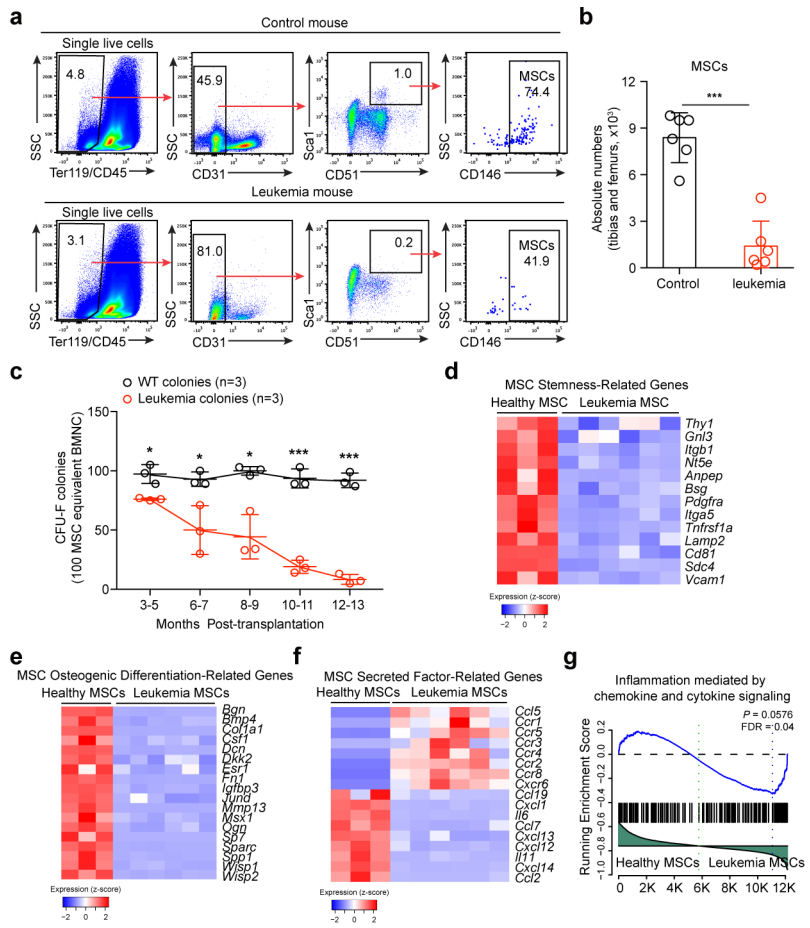

Fig.1 Impaired BM MSCs in mice with NrasG12D mutation-induced leukemia

CD45.2$^+$ BMNC from LSL *Nras*/+; *Vav-Cre* mice (NV mice) were sorted and transplanted into sublethally irradiated (6.5 Gy) individual recipients (CD45.1 strain) with a cell dose of 0.3 million per recipient. For control recipient mice (CD45.1 strain), 0.3 million sorted CD45.2$^+$ BMNC from WT mice were transplanted. **(a)** Gating strategies for BM MSCs. MSCs were defined as Ter119$^-$ CD45$^-$CD31$^-$Sca1$^+$CD51$^+$CD146$^+$. Plots from one representative control mouse (CD11b$^+$% in PB = 10%) and one leukemia-bearing mouse (CD11b$^+$% in PB > 60%) of six mice of each group were shown. The nucleated cell mixtures of BM and compact bones were prepared for flow cytometry analysis of MSCs. **(b)** Statistical analysis of the absolute numbers of MSCs in tibias and femurs

651 from control and leukemia-bearing mice. ***p < 0.001. Unpaired Student's t-test (two-tailed).
652 Data are represented as mean ± SD (n = 6 mice for each group). **(c)** Kinetic analysis of functional
653 MSCs in CFU-F assay. Total BMNC equivalent to 100 MSCs calculated by the percentages of
654 MSCs in individual BMNC samples by flow cytometry analysis. For each time point, BMNC of
655 three mice in each group were analyzed. *p < 0.05, ***p < 0.001. Unpaired Student's t-test (two-
656 tailed). Data are represented as mean ± SD. **(d)** Heatmaps of MSC stemness-related genes
657 differentially expressed between healthy MSCs and MSCs from leukemia-bearing mice (padj <
658 0.05, fold change > 1.6). One thousand sorted MSCs ($Ter119^{-}CD45^{-}CD31^{-}Sca1^{+}CD51^{+}$) from the
659 nucleated cell mixtures of BM and compact bones of leukemia-bearing mice and control mice were
660 used as each cell sample input for RNA-Seq. Leukemia-bearing mice ($CD11b^{+}$% in PB = 35%-
661 45%) and control mice ($CD11b^{+}$% in PB = 10-15%). The expression value (DESeq2 normalized
662 counts) of each gene was converted to z-score values (red, high; blue, low), and the heatmaps were
663 plotted by gplots (heatmap.2). Columns represent the indicated cell subsets in nine MSC samples
664 (Healthy MSCs from control mice: n = 3, MSCs from leukemia-bearing mice: n = 6). **(e)** Heatmaps
665 of osteogenic differentiation-related genes differentially expressed between healthy MSCs and
666 MSCs from leukemia-bearing mice (padj < 0.05, fold change > 2). The expression value (DESeq2
667 normalized counts) of each gene was converted to z-score values (red, high; blue, low), and the
668 heatmaps were plotted by gplots (heatmap.2). Columns represent the indicated cell subsets in nine
669 MSC samples (Healthy MSCs: n = 3, MSCs from leukemia-bearing mice: n = 6). **(f)** Heatmaps of
670 MSC secreted factor-related genes differentially expressed between healthy MSCs and MSCs from
671 leukemia-bearing mice (padj < 0.05, fold change > 2). The expression value (DESeq2 normalized
672 counts) of each gene was converted to z-score values (red, high; blue, low), and the heatmaps were
673 plotted by gplots (heatmap.2). Columns represent the indicated cell subsets in nine MSC samples

(Healthy MSCs: n = 3, MSCs from leukemia-bearing mice: n = 6). **(g)** GSEA of the inflammation mediated by chemokine and cytokine signaling in healthy MSCs and MSCs from leukemia-bearing mice. DESeq2 normalized values of the expression data were used for GSEA analysis.

Fig. 2

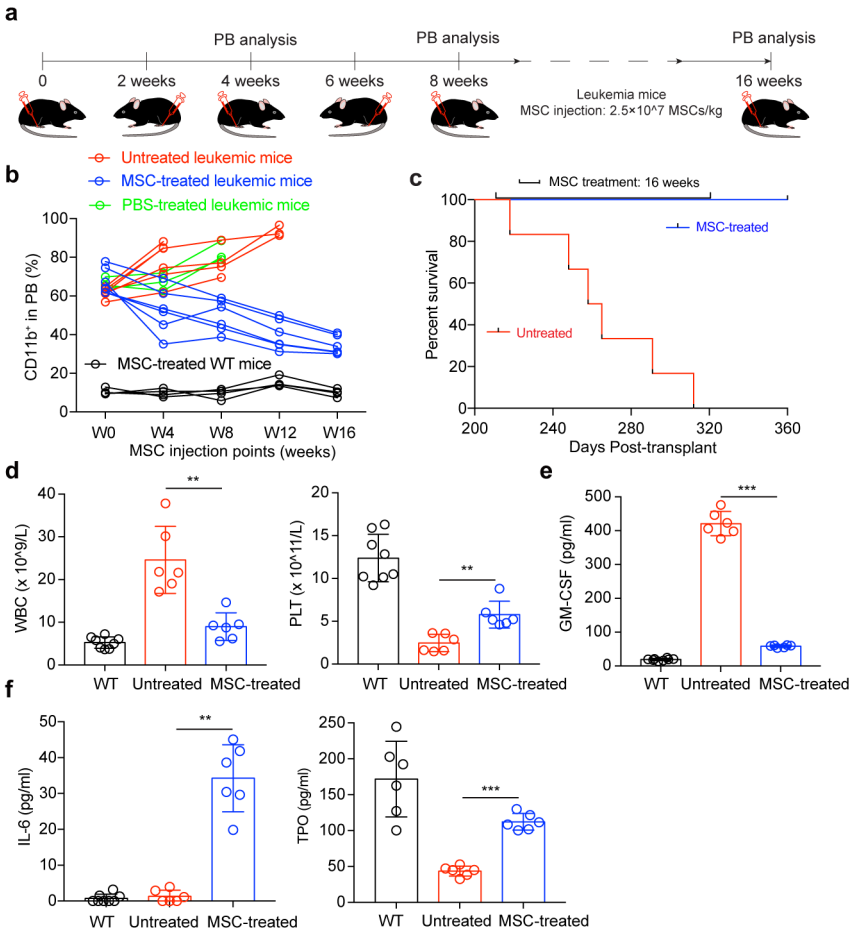

Fig.2 Intra-BM transfusion of donor MSCs prolongs survival of leukemia-bearing mice

(a) Schematic diagram of MSC transfusion strategy. The donor MSCs prepared for transfusion were isolated from the compact bone and BMNC of three to four-week-old healthy GFP mice. The isolated MSCs were expanded *in vitro*, and the secondary passage products were used for transfusion. Leukemia-bearing mice with severe tumor burden ($CD11b^+$% in PB > 60%) were treated by intra-bone-marrow transfusion of donor MSCs. WT mice were treated by the same procedure as treatment control, and leukemia-bearing mice without MSC treatment were used as untreated controls. A dose of 2.5 × 10^7 MSCs/kg in 20 μl DPBS were delivered into the tibia cavity using 29-gauge needle. Every tibia was treated once per month by switching the injection site every other dose. **(b)** Kinetic analysis of tumor burden ($CD11b^+$) of MSC-treated leukemia-

bearing mice. The time window of MSC treatment is from 0 weeks (W0, treatment starting time) to 16 weeks (W16). Flow cytometry analysis of tumor burden ($CD11b^{+}$) in PB was performed monthly. Untreated leukemia-bearing mice were used as disease control (red line), PBS-treated leukemia-bearing mice were used as injected control (green line), and MSC-treated WT mice were used as treatment control (black line). Untreated leukemia-bearing mice: n = 6; PBS-treated leukemia-bearing mice: n = 3; MSC-treated leukemia-bearing mice (blue line): n = 6; MSC-treated WT mice: n = 4. **(c)** Kaplan-Meier survival of MSC-treated leukemia-bearing mice. Kaplan-Meier survival curves of untreated (n = 6, Median survival = 261.5 days) and MSC-treated (n = 6, Median survival = 360 days) leukemia-bearing mice were shown. The untreated leukemia-bearing mice from the same batch were used as control (red line). Log-rank (Mantel-Cox) test: $p < 0.001$. **(d)** Statistical analysis of white blood cells (WBC) and platelets (PLT) counts in PB of WT mice, untreated leukemia-bearing mice, and MSC-treated leukemia-bearing mice at week nine since the MSC treatment. **p < 0.01. One-way ANOVA test. Data are represented as mean ± SD (n =6-8 mice for each group). **(e)** ELISA of GM-CSF levels in PB serum. Serum prepared from 200 μL PB of individual WT mice (n=8), untreated leukemia-bearing mice (Untreated, n=6) and MSC-treated leukemia-bearing mice (MSC-treated, n=6) eight weeks post MSC treatment. ***p < 0.001. One-way ANOVA test. Data are represented as mean ± SD. **(f)** ELISA of IL-6 and TPO levels in PB serum. Serum prepared from 200 μL PB of individual WT mice (n=8), untreated leukemia-bearing mice (Untreated, n=6) and MSC-treated leukemia-bearing mice (MSC-treated, n=6) eight weeks post MSC treatment. **p < 0.01, ***p < 0.001. One-way ANOVA test. Data are represented as mean ± SD.

Fig. 3

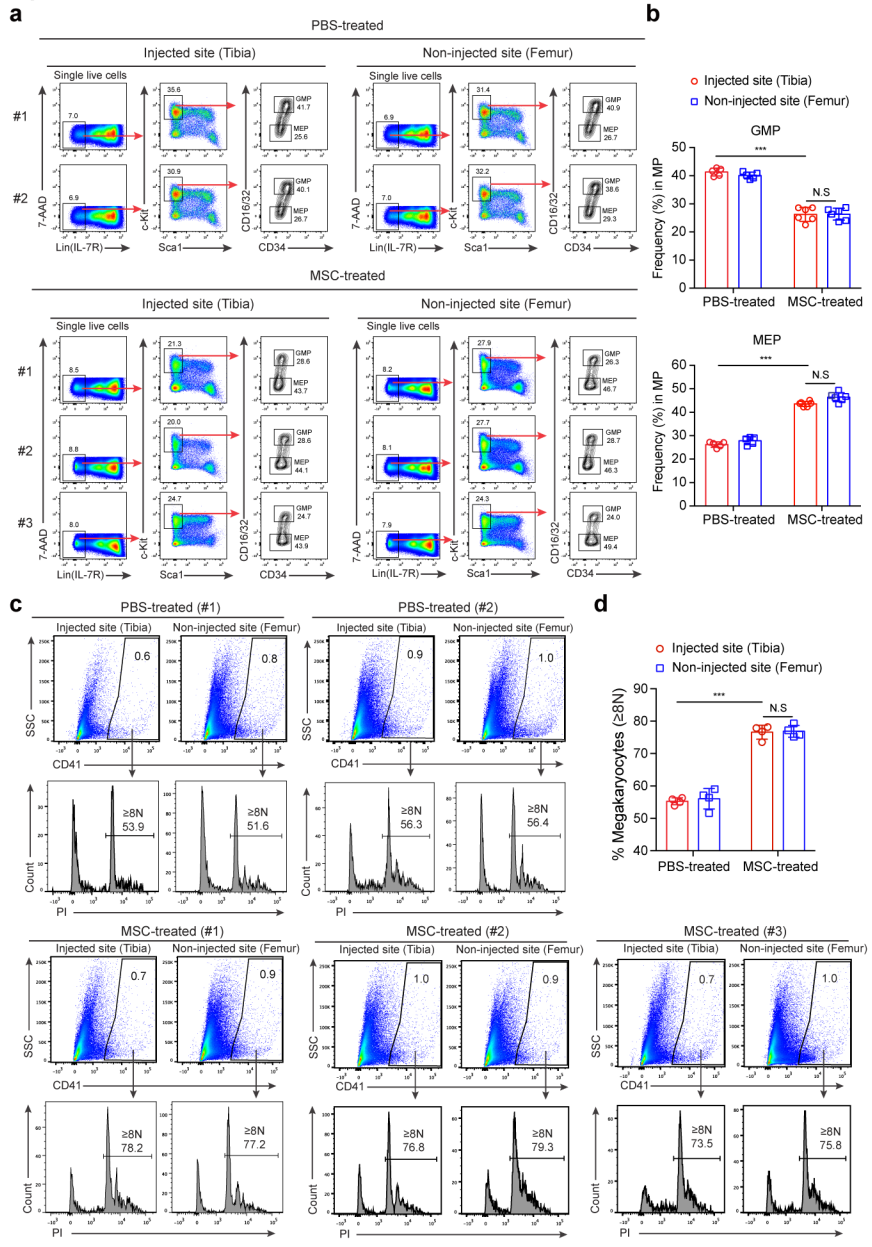

Fig.3 Systemically re-balanced myeloid lineage progenitor cells and systemically activated megakaryocytes in MSC-treated leukemia-bearing mice

(a) Ratios of myeloid progenitor subpopulations in MSC- and PBS-treated leukemia-bearing mice. Total bone marrow nucleated cells from the MSC-injected site (tibia) and non-injected site (femur) of each leukemia-bearing mouse (n=3), and PBS-injected site (tibia) and non-injected site (femur) of each leukemia-bearing mouse (n=2) four weeks post MSC/PBS treatment. GMP

(granulocyte/macrophage progenitors): $Lin^{-}IL\text{-}7R^{-}Sca1^{-}c\text{-}Kit^{+}CD34^{+}CD16/32^{high}$; MEP (megakaryocyte/erythroid progenitors): $Lin^{-}IL\text{-}7R^{-}Sca1^{-}c\text{-}Kit^{+}CD34^{-}CD16/32^{-}$. **(b)** Statistical analysis of myeloid progenitor components (GMP and MEP) in the injected site (tibia) and non-injected site (femur) of each PBS-treated leukemia-bearing mouse and MSC-treated leukemia-bearing mouse four weeks post-MSC treatment. ***$p < 0.001$. One-way ANOVA test. Data are represented as mean ± SD (n = 5-6 mice for each group). **(c)** Activation analysis of megakaryocytes in MSC- and PBS-treated leukemia-bearing mice. Plots from two representative PBS-treated leukemia-bearing mice and three representative MSC-treated leukemia-bearing mice four weeks post MSC treatment were shown. Percentages of mature megakaryocytes with 8N and greater ploidy (≥8N) were shown. **(d)** Statistical analysis of the percentages of mature megakaryocytes (≥8N). ***$p < 0.001$, N.S indicates non-significant. One-way ANOVA test. Data are represented as mean ± SD (n = 4 mice for each group).

Fig. 4

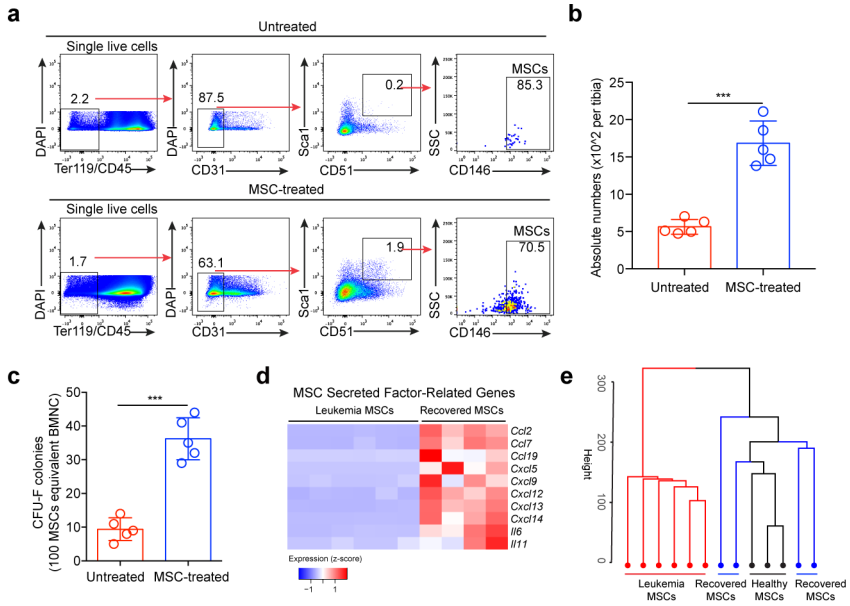

Fig.4 Characterization of recovered host MSCs from MSC-treated leukemia-bearing mice

(a) Flow cytometry analysis of recovered host MSCs in leukemia-bearing mice eight weeks post MSC treatment. Tibias of MSC-treated leukemia-bearing mice eight weeks after the first dose MSC treatment were analyzed. Plots of one representative mouse from each group were shown. MSCs were defined as $Ter119^{-}CD45^{-}CD31^{-}Sca1^{+}CD51^{+}CD146^{+}$. The nucleated cell mixtures of BM and compact bones were prepared for flow cytometry analysis of MSCs. **(b)** Statistical analysis of the absolute numbers of host MSCs (GFP^{-}, host-derived MSCs) in tibias from untreated and MSC-treated leukemia-bearing mice. ***$p < 0.001$. Unpaired Student's t-test (two-tailed). Data are represented as mean ± SD (n = 5 mice for each group). **(c)** Statistical analysis of CFU-F colonies. The numbers of colonies of each group were counted after Giemsa staining. ***$p < 0.001$. Unpaired Student's t-test (two-tailed). Data are represented as mean ± SD (n = 5 mice for each group). **(d)** Heatmaps of MSC secreted factor-related genes differentially expressed between MSCs from leukemia-bearing mice and recovered MSCs (padj < 0.05, fold change > 1.4). One thousand sorted MSCs ($Ter119^{-}CD45^{-}CD31^{-}Sca1^{+}CD51^{+}$) from the nucleated cell mixtures of BM

and compact bones of leukemia-bearing mice and MSC-treated leukemia-bearing mice were used as each cell sample input for RNA-Seq. Recovered MSCs were isolated from tibias of MSC-treated leukemia-bearing mice eight weeks after the first dose MSC treatment. The expression value (DESeq2 normalized counts) of each gene was converted to z-score values (red, high; blue, low), and the heatmaps were plotted by gplots (heatmap.2). Columns represent the indicated cell subsets in ten MSC samples (MSCs from leukemia-bear mice: n = 6, Recovered MSCs: n = 4). **(e)** Unsupervised hierarchical clustering of RNA-Seq data of MSCs from leukemia-bearing mice, healthy MSCs and recovered MSCs (GFP^-, recipient-derived). For each RNA-Seq sample, one thousand MSCs from leukemia-bearing mice, healthy mice, and MSC-treated leukemia-bearing mice were sorted and analyzed (n = 3-6). The raw reads (fastq files) from RNA-Seq were aligned to mouse genome by Tophat2 package, and further normalized by Cufflinks. Unsupervised hierarchical clustering was conducted by factoextra R package.

Fig. 5

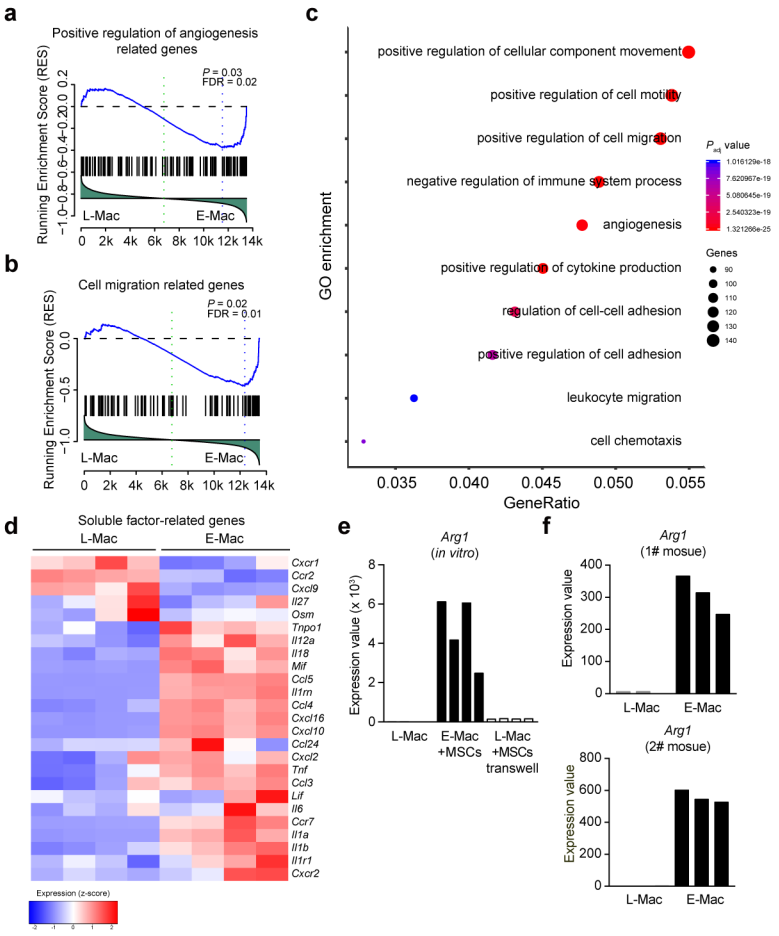

Fig.5 Characterization of MSC-reprogrammed BM resident macrophages isolated from leukemia-bearing mice

(a) Gene set enrichment analysis (GSEA) of the positive regulation of angiogenesis in L-Mac and E-Mac. L-Mac indicates leukemia macrophages. E-Mac indicates MSC-reprogrammed leukemia macrophages, which were co-cultured with MSCs *in vitro* for 12 h. DESeq2 normalized values of the expression data were used for GSEA analysis. **(b)** Gene set enrichment analysis (GSEA) of the cell migration related genes in L-Mac and E-Mac. DESeq2 normalized values of the expression data were used for GSEA analysis. **(c)** Gene ontology (GO)–enrichment analysis of the 3277 differentially expressed genes between L-Mac and E-Mac: each symbol represents a GO term (noted in the plot); color indicates adjusted P value (padj (significance of the GO term)), and

symbol size is proportional to the number of genes. **(d)** Heatmaps of soluble factor-related genes in MSC-reprogrammed leukemia macrophages. The expression value (DESeq2 normalized counts) of each gene was converted to z-score value (red, high; blue, low). The heatmaps were plotted by gplots (heatmap.2). Columns represent the indicated macrophage sample replicates (L-Mac: n = 4 biological replicates; E-Mac: n = 4 biological replicates). **(e)** RNA-Seq analysis of *Arg1* in leukemia macrophages co-cultured with MSCs *in vitro*. L-Mac indicates leukemia macrophages. E-Mac (+MSCs) indicates MSC-reprogrammed leukemia macrophages, which were co-cultured with MSCs *in vitro* for 12 h. L-Mac (+MSCs transwell) indicates leukemia macrophages, which were transwell co-cultured with MSCs *in vitro* for 12 h. Y-axis indicates the expression value. The expression value (DESeq2 normalized counts) of each gene was illustrated by graphpad. Each column represents a replicate. **(f)** RNA-Seq analysis of *Arg1* in leukemia macrophages sorted from MSC-treated leukemia mice *in vivo*. Leukemia macrophages ($CD11b^{+}F4/80^{+}$) were sorted from the injected site (MSC-treated tibia) and non-injected site (untreated femur) of leukemia mice 12 h post-treatment. Y-axis indicates the expression value. The expression value (DESeq2 normalized counts) of each gene was illustrated by graphpad. Each column represents a replicate.

Fig. 6

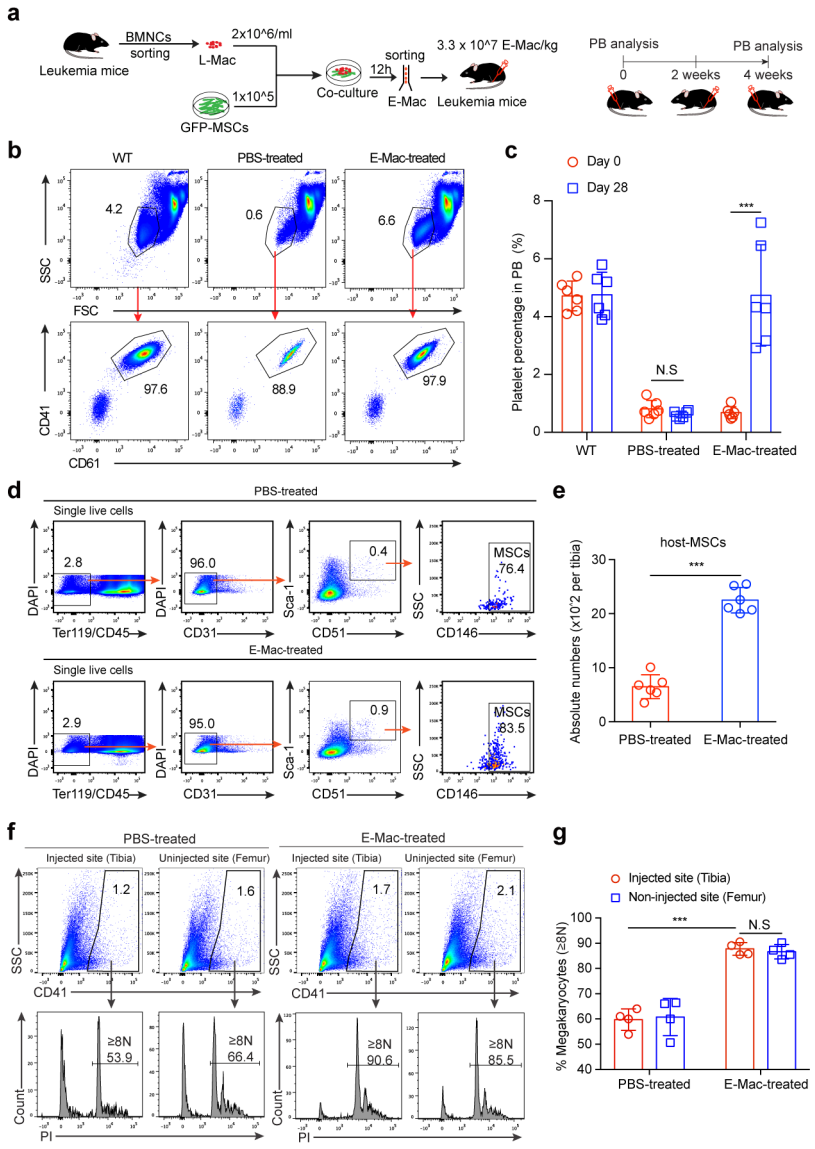

Fig.6 Intra-bone-marrow transfusion of MSC-reprogrammed macrophages largely rescues the therapeutic effects of MSC-treatment in leukemia mice

(a) Schematic diagram of MSC-reprogrammed macrophages transfusion strategy. 1 × 10^5 GFP^+ MSCs were seeded into each well of six-well plate. $CD11b^+$ leukemia cells were enriched from bone marrow of leukemia mice with severe tumor burden ($CD11b^+$% in PB > 60%). Then 2 × 10^6 $CD11b^+$ leukemia cells were directly co-cultured with MSCs. After 12 hours, leukemia macrophages ($CD11b^+F4/80^+$) were sorted for transfusion. Leukemia mice with severe tumor

790 burden were treated by intra-bone-marrow transfusion of PBS or MSC-reprogrammed leukemia
791 macrophages (E-Mac). A dose of 3.3 × 10^7 E-Mac/kg in 20 μl PBS were delivered into the tibia
792 cavity using 29-gauge needle. Every tibia was treated once per two weeks by switching the
793 injection site every other dose. Analysis of platelets and $CD11b^+$ cells in PB was performed
794 monthly. **(b)** Representative dot plots of platelet populations and quantitative gating, as identified
795 by CD41 and CD61 staining in PB of WT mice and PBS/E-Mac treated leukemia mice. After 4
796 weeks of PBS/E-Mac treatment, PB of leukemia mice with PBS/E-Mac treatment was analyzed.
797 **(c)** Statistical analysis of platelets in PB of leukemia-bearing mice treated with PBS or E-Mac.
798 ***$p < 0.01$. N.S indicates non-significant. One-way ANOVA test. Data are represented as mean
799 ± SD (n = 6 mice for each group). **(d)** Flow cytometry analysis of MSCs in leukemia-bearing mice
800 post PBS/E-Mac treatment. Tibias of PBS/E-Mac treated leukemia mice at week five since the
801 first dose of PBS/E-Mac treatment were analyzed. MSCs were defined as $Ter119^-CD45^-CD31^-$
802 $Sca1^+CD51^+CD146^+$. The nucleated cell mixtures of BM and compact bones were prepared for
803 flow cytometry analysis of MSCs. **(e)** Statistical analysis of the absolute numbers of host MSCs in
804 tibias from PBS/E-Mac treated leukemia mice. ***$p < 0.001$. Unpaired Student's t-test (two-
805 tailed). Data are represented as mean ± SD (n = 6 mice for each group). **(f)** $CD41^+$ megakaryocytes
806 from BM of MSC-injected site (tibia) and non-injected site (femur) were analyzed for DNA
807 content. Plots from representative PBS-treated and E-Mac-treated leukemia mice four weeks post
808 PBS/E-Mac treatment were shown. Percentages of mature megakaryocytes with 8N and greater
809 ploidy (≥8N) were shown. **(g)** Statistical analysis of the percentages of mature megakaryocytes
810 (≥8N) of $CD41^+$ BM megakaryocytes. ***$p < 0.001$. One-way ANOVA test. Data are represented
811 as mean ± SD (n = 4 mice for each group).

Fig. 7

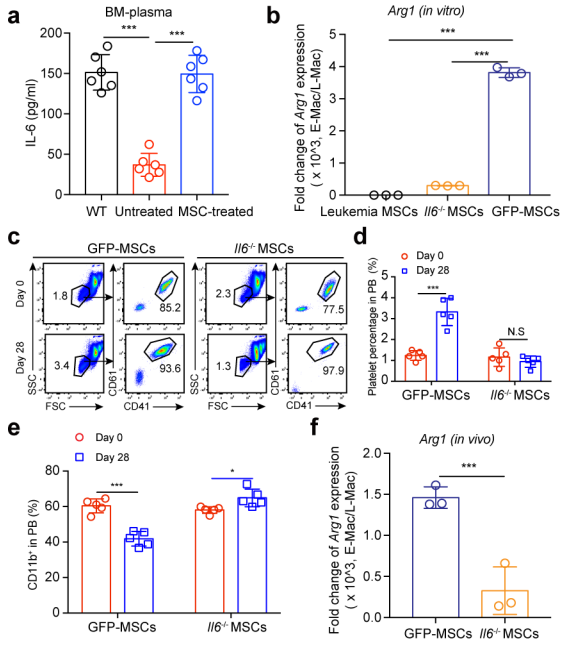

Fig.7 *Il6*$^{-/-}$ MSCs neither reprogram macrophages from leukemia-bearing mice nor suppress leukemia

(a) ELISA of IL-6 levels in BM plasma. The BM plasma from WT mice, untreated leukemia-bearing mice and MSC-treated leukemia-bearing mice eight weeks post MSC treatment were analyzed. The BMNC of tibias and femurs were flushed out using 2 ml PBS, then the supernatants of each sample were collected for ELISA. ***p < 0.001. One-way ANOVA test. Data are represented as mean ± SD (n = 6 mice). **(b)** Q-PCR of *Arg1* expression levels in macrophages from leukemia-bearing mice after co-culture with different sources of MSCs *in vitro*. Macrophages from leukemia-bearing mice were co-cultured with MSCs from leukemia-bearing mice, *Il6*$^{-/-}$ MSCs or GFP-MSCs *in vitro* for 12 h, separately. Then, one hundred thousand E-Mac (CD11b^{+}F4/80^{+}) were sorted and were analyzed the expression of *Arg1*. Y-axis shows the fold changes of E-Mac/L-Mac in each group. ***p < 0.001. One-way ANOVA test. Data are represented as mean ± SD (n = 3 repeats for each group). **(c)** Flow cytometry analysis of platelets in *Il6*$^{-/-}$ MSC-treated leukemia-bearing mice. Representative dot plots of platelet populations and quantitative gating, as identified

by CD41 and CD61 staining in PB of GFP-MSC- or *Il6*$^{-/-}$ MSC-treated leukemia-bearing mice. PB of leukemia-bearing mice was analyzed at week-0 and week-4 post-treatment with GFP-MSCs or *Il6*$^{-/-}$ MSCs. **(d)** Statistical analysis of platelets (PLT) in PB of leukemia-bearing mice treated with GFP-MSCs or *Il6*$^{-/-}$ MSCs. ***$p < 0.01$. N.S indicates not significant. One-way ANOVA test. Data are represented as mean ± SD (n = 5 mice for each group). **(e)** Statistical analysis of tumor burden ($CD11b^{+}$) in PB of leukemia-bearing mice treated with GFP-MSCs or *Il6*$^{-/-}$ MSCs. ***$p < 0.01$. N.S indicates non-significant. One-way ANOVA test. Data are represented as mean ± SD (n = 5 mice for each group). **(f)** Q-PCR of *Arg1* expression levels in macrophages isolated from *Il6*$^{-/-}$ MSC-treated leukemia-bearing mice. One hundred thousand leukemia macrophages ($CD11b^{+}F4/80^{+}$) were sorted from the MSC-injected site (MSC-treated tibia) and non-injected site (femur) of leukemia-bearing mice 12h post-treatment. Y-axis shows the fold changes of E-Mac/L-Mac in each group. ***$p < 0.001$. Unpaired Student's t-test (two-tailed). Data are represented as mean ± SD (n = 3 mice for each group).